Archives of Hydro-Engineering and Environmental Mechanics 70 (2023), pp. 1–16, doi: 10.2478/heem-2023-0001

sciendo

ARCHIVES OF HYDRO-ENGINEERING AND ENVIRONMENTAL MECHANICS

Published since 1954

ISSN 1231–3726

On the Hydraulic Characteristics of Submerged Flow over Trapezoidal-Shaped Weirs

Yebegaeshet T. Zerihun

David & James – Engineering and Environmental Consultancy, 204 Albion Road, Vic 3350, Australia;
e-mail: zyebegaeshet@gmail.com

(Received 25 November 2022; revised 29 January 2023)

Abstract. Subcritical flows over highway and railway embankments, commonly encountered during flood events, can be treated like submerged flows over trapezoidal-shaped weirs. In earlier studies, the equation of the submerged-flow discharge for such types of weirs was developed as a function of the degree of submergence and free-flow discharge. However, the application of this equation in practice requires a pre-determined discharge from experiments performed under free-flow conditions. In this study, a discharge equation was deduced from the streamwise momentum balance equation, which overcomes the drawback of the previous approaches. The results of the validation demonstrated that the proposed equation is capable of predicting the submerged-flow discharge of a trapezoidal-shaped weir within ±6.0% of the measured value. Furthermore, the most prominent features of the submerged overflows were examined by systematically analyzing the experimental data. For such flows, the free-surface and bed-pressure profiles are self-similar only over the upstream face of the weir. Results of this investigation confirmed that the degree of submergence and the slope of the downstream weir face significantly affect the characteristics of the submerged flow, but the effect of the latter on the non-modular discharge is marginal.

Key words: submerged-flow discharge, hydraulic structure, trapezoidal-shaped weir, flow measurement, subcritical flow, modular limit

1. Introduction

Submerged flow occurs when the flow passes over the weir in a subcritical state. For such tailwater-controlled conditions, the submergence ratio S (= t/h, where h is the overflow depth, and t is the crest-referenced tailwater depth) exceeds the modular limit of the flow. The modular limit is the value of the submergence ratio that corresponds to the incipient-submergence tailwater depth for which the approach flow is not yet submerged (Hager 2010, p. 359). The characteristics of the overflows, surface roughness, and geometry of the weir significantly affect the modular limit. Its value decreases with increasing roughnesses of the weir surface and approach channel (Kindsvater 1964) and increases as the downstream-face slope flattens (Thomas

1966). The influence of the latter factor is the result of the highly dependent of the dynamic characteristics of the overflow on the slope of the downstream weir face (Zerihun 2020). It is apparent that a variation of the relative overflow head ζ (= H_0/L, where H_0 is the upstream crest-referenced energy head of a modular flow, and L is the crest length in a streamwise direction) results in a change in the degree of the curvature of the overflow and thus a modification of the modular limit characteristics. As noted by Bos (1989, p. 89) and Zerihun (2004), the modular limit of a weir decreases as the curvature of the streamline increases. In other word, a trapezoidal broad-crested weir ($0.07 \leq \zeta \leq 0.50$) has a higher modular limit compared to a short-crested type of similar weir ($0.50 \leq \zeta \leq 1.50$ to 1.80).

Subcritical flow over highway and railway embankments, which usually encounters during flood events, can be analyzed by the hydraulic theory of submerged flows over trapezoidal-shaped weirs. The dynamics of submerged flow over such weirs have been experimentally studied by many researchers (Prawel 1958, Smith 1959, Kindsvater 1964, Thomas 1966, Fritz and Hager 1998, Zerihun 2004). Prawel (1958) conducted tests on embankment-shaped weirs discharging under free- and submerged-flow conditions. The weirs had upstream- and downstream-face slopes of 26.57° and a crest length of 1016 mm. The influence of embankment shape on the characteristics of discharge was examined. Likewise, Smith (1959) carried out experiments on submerged flows over trapezoidal-shaped weirs. He considered two symmetrical weirs, each having a crest length of 152 mm and slopes of 45° and 26.57° for both the upstream and downstream faces. For both weirs, empirical equations for the coefficient of the submerged-flow discharge were developed using measurements with overflow depths less than 72 mm. For such small depths, however, the study did not account for the effects of viscosity and surface tension on weir flow. Kindsvater (1964) investigated the hydraulic characteristics of free and submerged flows over embankment-shaped weirs with weir heights ranging from 89 to 357 mm. The investigation was mainly based on compiled experimental data from the literature. Thomas (1966) studied the submerged-flow characteristics of trapezoidal-shaped weirs with varying downstream-face slopes. His models had an upstream-face slope of 26.57° and crest lengths varying from 253 to 610 mm. The effects of the variations of such weir geometry parameters on the characteristics of discharge were analyzed. In a similar study on submerged flows over triangular- and rectangular-shaped weirs, Abou-Seida and Quraishi (1976) examined the effects of rounding the upstream corner and of the slope of the upstream face on submerged-flow discharge. Recently, Fritz and Hager (1998) conducted experiments to examine the characteristics of the subcritical flow downstream of the submerged weirs. They considered trapezoidal-shaped weirs with both upstream and downstream faces sloped at 26.57°, and their crest length varied from 0 to 300 mm. The study showed a considerable improvement over the aforementioned earlier works by generalizing the global characteristics of the submerged flow downstream of the weirs. However, the key characteristics of the subcritical overflow have not been investigated in detail. Zerihun (2004) also carried

out a series of experiments on flows over trapezoidal-shaped weirs with a symmetrical face slope of 26.57°. The experiments were conducted on weirs having a height of 150 mm and crest lengths of 100, 150, and 400 mm; they were planned to fill in some of the more obvious knowledge gaps in the area of weir hydraulics. Both studies (Fritz and Hager 1998, Zerihun 2004) analyzed the effects of the relative overflow head on the hydraulic performance of trapezoidal-shaped weirs under free- and submerged-flow conditions. Furthermore, higher-order numerical models were widely applied to explore the submerged-flow characteristics of trapezoidal- and ogee-shaped weirs (e.g., Huang and Ng 2007, Zerihun and Fenton 2007, Pedersen et al 2018, Qian et al 2021). The performance of these types of models has been fine-tuned by using the data of experimental studies that aimed to examine the structure of the flow field (see, e.g., Zerihun 2004, Peltier et al 2018, Biegowski et al 2020, Karim and Mohammed 2020).

In addition to analyzing the flow structure, several studies (e.g., Kindsvater 1964, Thomas 1966, Abou-Seida and Quraishi 1976, Hager 1994a, Hager and Schwalt 1994, Fritz and Hager 1998, Zerihun 2004, Hakim and Azimi 2017) employed an empirical method based on the analysis of experimental data to deduce the equation of the submerged-flow discharge as a function of the degree of submergence and free-flow discharge. However, the application of the resulting equation requires an additional measurement of free-flow discharge. As an alternative, Skogerboe et al (1966) developed a semi-empirical discharge equation. Similar to the Smith (1959) equations, their equation only directly yields the submerged-flow discharge of a trapezoidal broad-crested weir.

The above review demonstrates that most of the experimental works have been performed to provide insights into both the macroscopic structure and the discharge characteristics of submerged flows over trapezoidal-shaped weirs. Systematic investigations of the salient features of a submerged flow over such weirs have not been thoroughly carried out. By analyzing experimental data from the literature, the nature of the free-surface and bed-pressure profiles under different degrees of submergence will be investigated here. Furthermore, a discharge equation for submerged-flow conditions will be developed by using the momentum principle in a streamwise direction. The proposed equation does not require a prior knowledge of the free-flow discharge; hence, it is easy to apply to a real-life flow problem. Such a physically-based equation can provide a realistic solution to engineering problems related to the prediction of discharge over an embankment-shaped weir from post-flood field observations. As an additional factor, the variation of the downstream-face slope is considered, and its effect on submerged-flow characteristics will also be examined. In the following sections, the development of the discharge equation and the results of the analysis of the experimental data will be presented.

2. Methodology

In a streamwise direction, the momentum principle was applied to develop a discharge equation for submerged-flow conditions. This equation was first calibrated and then validated using a large set of experimental data from the literature (Prawel 1958, Thomas 1966, Zerihun 2004). The data were further analyzed to examine the effects of submergence on the local flow characteristics of a trapezoidal-shaped weir. Table 1 summarizes the flow conditions of the selected experimental studies. Also, the Froude number of the approach flow, F_{r0}, is estimated based on the flow parameters at the upstream end section. As shown in Table 1, it is relatively low due to the submerged overflow situation.

Table 1. Summary of scope of experimental studies of submerged flows over trapezoidal-shaped weirs with symmetrical and asymmetrical face slopes

Experiments	S (%)	Side slope	$h/(h + w)$	F_{r0}
1. Prawel (1958) Series (Models 2 and 7)	89–99	$\theta = \varphi = 26.57°$	0.10–0.38	0.02–0.11
2. Thomas (1966) Series (Models A-I)	80–99	$\theta = 26.57°$ and $14.04° \leq \varphi \leq 45°$	0.15–0.57	0.03–0.18
3. Zerihun (2004) Series (Models Pn10, Pn15, and Pn40)	84–98	$\theta = \varphi = 26.57°$	0.24–0.46	0.06–0.18

The presence of size-scale effects can affect the physical processes governing the dynamics of free-surface flow, thus making an accurate prediction of the features of a prototype flow such as discharge, pressure, and energy dissipation using laboratory data more challenging. In this study, size-scale effects due to viscosity and surface tension on the experimental data were examined based on the general criteria suggested by Hager (1994b) and Curtis (2016). Accordingly, these effects were eliminated from the final results by averting measurements with overflow depths less than 50 mm. Additionally, the flow data of trapezoidal-shaped weirs with a minimum structural height of 150 mm were considered to reduce high measurement uncertainties. The weir models of the selected experiments had a relative width λ_B (= B/L, where B is the width of the weir) value between 0.75 and 3, which is greater than the recommended lower limit value of 0.20 (Bos 1989, p. 147). Hence, the reported experimental data are free of the effects of boundary-layer growth on the sidewalls. It is worth noting that all measurements were taken along the centerline of the channels owing to the insignificant transverse variation of the overflow characteristics.

3. Submerged-Flow Discharge Equation

For a unit width of a rectangular channel, a control volume of fluid, which is bounded by the vertical sections at 1 and 2, the free surface, and the surfaces of the approach channel and weir, is shown in Fig. 1. Let U and F denote the mean streamwise velocity and horizontal force, respectively. Further, h_v stands for the velocity head of

the approach flow. The following assumptions are made in developing the discharge equation for a submerged trapezoidal-shaped weir: (1) the channel bed and the weir crest are both horizontal; (2) the boundary shear forces along the solid surface between Sections 1 and 2 are ignored; (3) the velocity distribution at Sections 1 and 2 is uniform; (4) the surface tension effects are ignored; and (5) the pressure distribution over the upstream face of the weir and at Section 2 is hydrostatic.

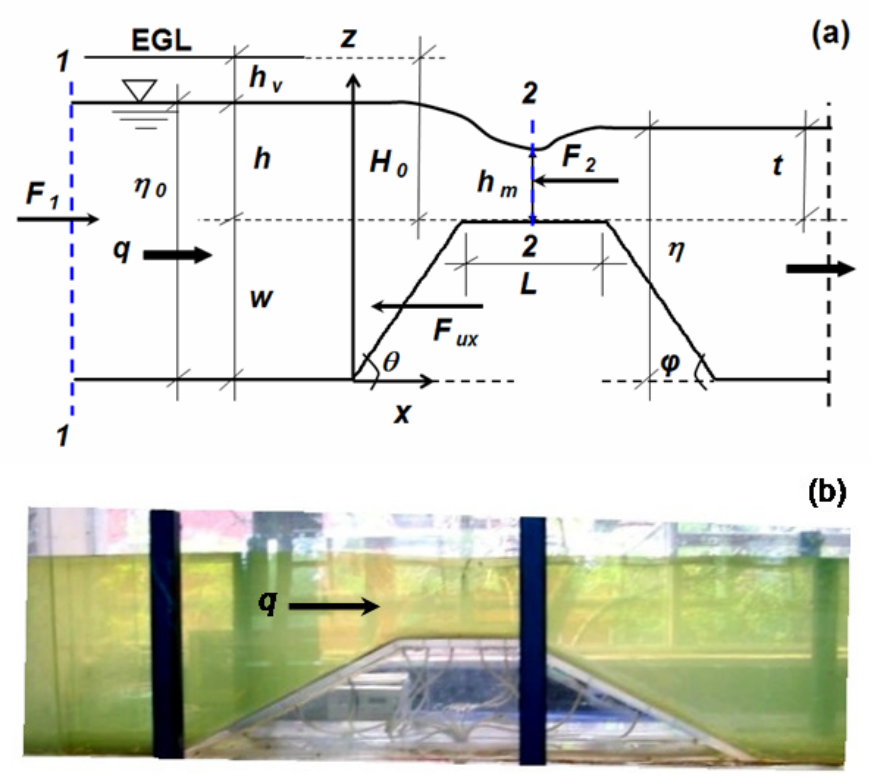

Fig. 1. (a) Definition sketch of subcritical flow over a trapezoidal-shaped weir; and (b) a broad-crested weir flow with a submergence ratio of 97% (photo taken from Zerihun (2004)). The slopes of the upstream and downstream faces are denoted by θ and φ, respectively, and EGL represents the energy grade line for steady flow. The origin of the Cartesian coordinates (x, z) is at the heel of the weir

Applying the momentum equation in the x-direction for the control volume in Fig. 1, one obtains

$$F_1 - (F_{ux} + F_2) = \frac{\gamma}{g} q\,(U_2 - U_1)\,, \tag{1}$$

where q is the discharge per unit width; γ is the unit weight of the fluid; F_{ux} is the horizontal component of the force of the upstream weir face on the fluid; and g is acceleration due to gravity. Subscripts 1 and 2 refer to parameters at the upstream and downstream sections of the control volume, respectively. Using the assumed hydrostatic pressure distribution, the expressions for the horizontal forces are obtained as follows:

$$F_1 = \frac{\gamma}{2}(h + w)^2, \tag{2}$$

$$F_2 = \frac{\gamma}{2}h_m^2, \tag{3}$$

$$F_{ux} = \gamma w\left(\sigma h + \frac{w}{2}\right), \tag{4}$$

where w is the height of the weir; h_m is the flow depth at the center of the weir crest; and σ is a correction factor for the effect of the drawdown of the free surface. This factor can be determined from flow depths measured at the heel and upstream end of the weir crest. Inserting Equations (2)–(4) into Equation (1) and simplifying the resulting expression using the continuity equation ($U_1(h + w) = U_2 h_m = q$) gives the following equation for the submerged-flow discharge:

$$\Phi = \frac{q}{\sqrt{gh^3}} = \Gamma_2\left[\frac{\Gamma_3\frac{h_m}{h}\left(\left(1.0 - \left(\frac{h_m}{h}\right)^2\right) + 2\Gamma_1(\Gamma_3 - 1)\right)}{2\left(\Gamma_3 - \frac{h_m}{h}\right)}\right]^{\frac{1}{2}}, \tag{5a}$$

$$\Gamma_1 = 1 - \sigma, \tag{5b}$$

$$\Gamma_2 = \mu_1\,(1 - S^{\mu_2})^{\mu_3}\,, \tag{5c}$$

$$\Gamma_3 = 1 + \frac{w}{h}, \tag{5d}$$

where Φ is the normalized submerged-flow discharge; μ_1, μ_2 and μ_3 are empirical constants; and Γ_2 is a coefficient to correct the deviation from the above simplifying assumptions and also accounts for the effect of the weir geometry. The degree of submergence predominantly affects the value of this coefficient. Its average values can be estimated from the experimental data using a non-linear optimization technique, which utilizes the generalized reduced gradient method (Lasdon et al 1974). Equation (5a) is restricted to submerged flow over a trapezoidal-shaped weir with $h \geq 50$ mm.

3.1. Estimation of Flow Parameters

For simplifying the computational procedures, empirical equations for σ and h_m/h were developed by analyzing experimental data for submerged flows over trapezoidal-shaped weirs. Fig. 2 shows the variation of σ with the submergence ratio S. At a lower

submergence ratio close to the modular limit, the free-surface profile over the weir crest possesses small curvatures near the edges, resulting in a value of $\sigma < 1.0$. However, increasing the submergence ratio ($S \rightarrow 1$) has the effect of changing this flow behavior into a nearly horizontal flow situation with $\sigma \cong 1.0$. The best-fit equation of σ for a subcritical weir flow is shown in Fig. 2. It is pertinent to note that this equation is limited to the ranges of the flow parameters provided in Table 1. The development of a similar equation for other weir geometries requires only the generation of additional data employing experimental studies.

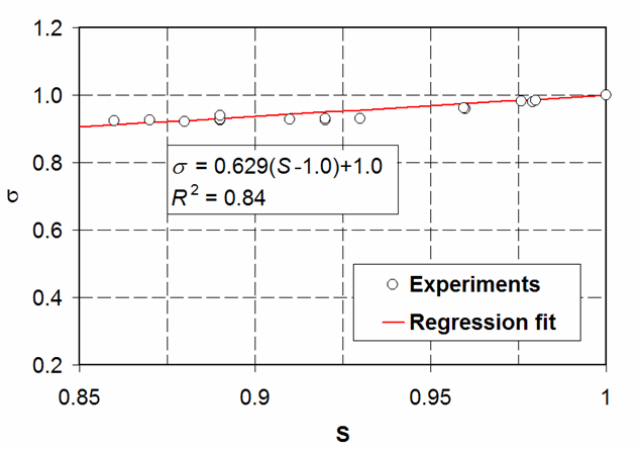

Fig. 2. Variation of the free-surface drawdown factor σ with the submergence ratio S

Apparently, the energy loss of a submerged flow is indirectly influenced by weir geometry such as weir face slopes and crest length. For instance, submerged flow over a rectangular-shaped weir experiences a higher energy loss and hence a lower modular limit compared to a similar weir with flatter upstream- and downstream-face slopes. For the type of weir considered, the relationship between the energy loss and the degree of submergence can be found through the application of an empirical approach, as was previously done by Skogerboe et al (1966). Fig. 3 depicts the variation of ψ (= log S) with the relative potential energy loss of the subcritical weir flow ω[= $(h - t)/h_m$]. As $S \rightarrow 1$, ω approaches zero, which corresponds to a deeply submerged-flow condition with a negligible energy loss. For the case considered here, the variation of ψ is approximated by a linear relationship with a coefficient of determination R^2 = 0.99, as shown in Fig. 3. Further manipulation of the regression equation yields

$$\frac{h_m}{h} = \frac{-0.367(1 - S)}{\psi}. \tag{6}$$

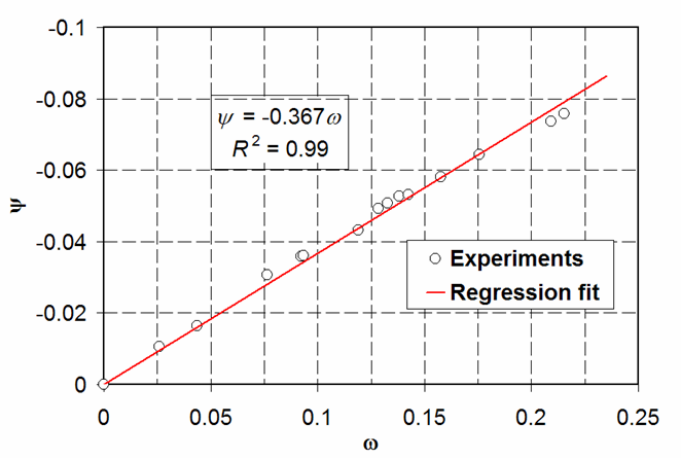

Fig. 3. The logarithmic submergence ratio ψ for subcritical flows over trapezoidal-shaped weirs as a function of the relative energy loss ω

The application of the above equation is limited to submerged flows over weirs with $\theta = 26.57°$ and $\varphi \leq 45.0°$. For other types of design geometries, the preceding method can be employed to develop structurally similar equations.

3.2. Verification of the Results

As described before, the value of Γ_2 was determined by calibrating Equation (5a) using the experimental data of Prawel (1958), Thomas (1966), and Zerihun (2004). In addition, the normalized discharge computed from the calibrated equation was verified using the remaining experimental data of Prawel (1958) and Thomas (1966). The results of the validation were also compared with the predictions of the previous semi-empirical equation proposed by Skogerboe et al (1966). Their equation for submerged flows over an embankment-shaped weir with upstream- and downstream-face slopes of 26.57° can be written as

$$\Phi = \frac{q}{\sqrt{gh^3}} = \frac{2.41h^{0.03}(1-S)^{1.53}}{(-\log S)^{1.20}\sqrt{g}}. \tag{7}$$

Figure 4 depicts the results of the calibration for submerged flows over trapezoidal-shaped weirs with varying downstream-face slopes. It compares the numerically computed normalized discharge, Φ_n, with the measured one, Φ_m. Note that most of the computed points collapsed close to the line of best fit, with a maximum root mean square error of 6.2%. Some of the optimal values of the empirical parameters are given in Table 2.

The performance of Equation (5a) was further examined by considering symmetrical and asymmetrical trapezoidal-shaped weirs. As shown in Fig. 5a, the agreement

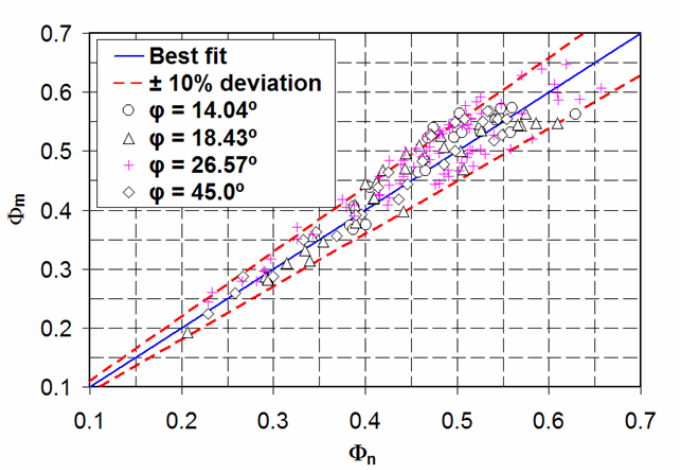

Fig. 4. Correlation between predicted and measured normalized discharges for submerged flows over trapezoidal-shaped weirs with an upstream-face slope $\theta = 26.57°$. The data of the test series of Model 7 from the Prawel (1958), part of Models A-I from the Thomas (1966), and part of the three models from Zerihun's (2004) experiments were used for calibration

Table 2. Typical calibrated values of the empirical constants for broad-crested weir flows

φ (deg)	L (mm)	μ_1	μ_2	μ_3
18.43	457	0.88	74.70	1.21
26.57	1016	0.82	55.30	0.40
45.0	610	0.80	80.65	1.25

between the validation results of the present method and the experimental data was relatively close, with a mean absolute relative error of 5.3%. For this test case, the results of the proposed method for a submerged-flow discharge were marginally better than the results of the earlier semi-empirical equation. Fig. 5b compares the computed normalized discharges with the experimental data for asymmetrical weirs. As can be seen, the present method satisfactorily predicted the submerged discharge irrespective of the steepness of the downstream weir face. The root mean square error of the computed points was less than 4%, and hence, these points fell in the error bandwidth of ±10%. Examination of the results also revealed that for the same value of S, the submerged-flow discharge increases with increasing the relative overflow head above the upper limit of the range of a broad-crested weir flow, as noted by Zerihun (2004). This is due to the fact that a short-crested weir generally requires less energy to discharge a given flow than a broad-crested type.

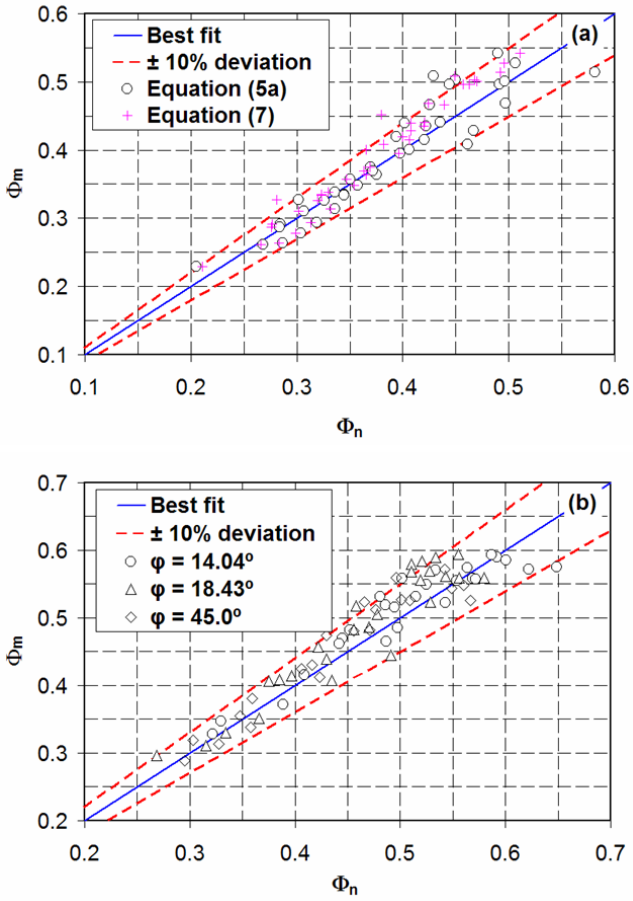

Fig. 5. Correlation between measured normalized discharges and simulated results for flows over trapezoidal-shaped weirs under submerged-flow conditions: (a) symmetrical weir; and (b) asymmetrical weir. The data of the test series of Model 2 from the Prawel (1958) and Models A-I from the Thomas (1966) experiments were used in (a) and (b), respectively

3.3. Effect of Downstream-Face Slope

For assessing the impact of the downstream-face slope on the discharge characteristics, the results of Equation (5a) for various values of relative weir height are plotted in Fig. 6. It can be seen from Fig. 6b that for a given weir height at larger overflow depths ($w/h \leq 0.5$), the submerged-flow discharge varies more gradually with S, especially for submergence ratio below 95%. A similar trend of discharge variation can also be seen for a flatter downstream-face slope. This is due to the fact that with a flatter slope, the energy-dissipating turbulent eddies in the downstream flow separation zone consume less energy. As a result, the flow attains a higher modular limit (Thomas 1966).

For a constant submergence ratio, increasing the side slope results in more large size energy-dissipating eddies in the recirculation zone near the channel bottom. The appearance of similar standing eddies behind a submerged sharp-crested weir was also reported by Rajaratnam and Muralidhar (1969). Consequently, the submerged weir gradually becomes hydraulically less efficient as the steepness of the slope increases (see Fig. 6a). In contrast, the free-flow discharge of a similar short-crested weir significantly increases as the slope of the downstream face increases (Zerihun 2020). Compared to the downstream-face slope, the effects of the degree of submergence on the discharge characteristics are more predominant. The results of the analysis for the effect of relative weir height on submerged discharge are consistent with the investigation results of Vennard and Weston (1943) and Prawel (1958) for submerged flows over a vertical sharp-crested weir and a highway embankment, respectively.

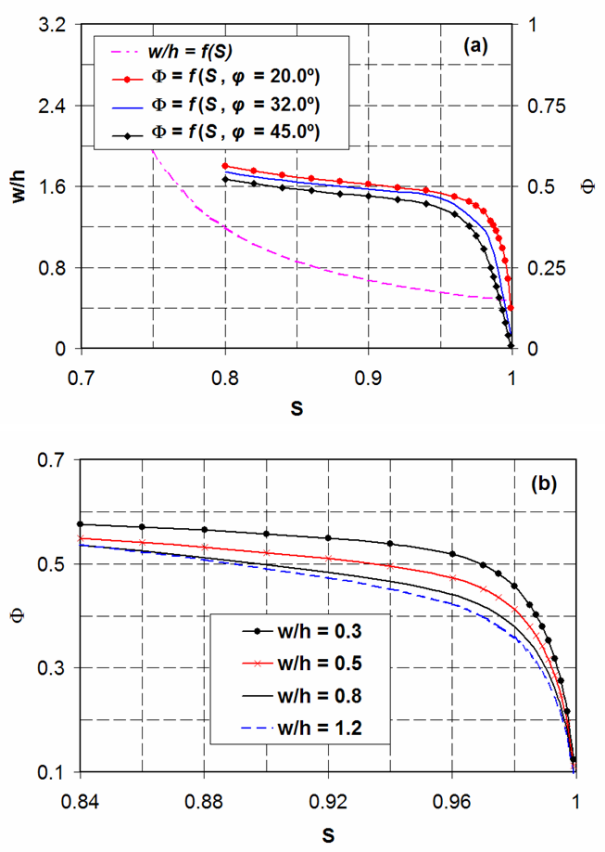

Fig. 6. (a) Variation of the submerged-flow discharge Φ with the submergence ratio S for various values of downstream-face slope φ and relative weir height w/h; and (b) the submerged-flow discharge of a weir with $\varphi = 20°$ as a function of S. $f(\,)$ stands for a functional relation

4. Characteristics of Subcritical Overflows

4.1. Free-Surface Profiles

The axial free-surface profile data from the experiments conducted by Zerihun (2004) were systematically analyzed. Fig. 7 depicts the normalized free-surface profile with $\Omega = \eta/\eta_0$ and $X = x/\eta_0$ for various degrees of submergence, where Ω is the normalized free-surface elevation, X is the non-dimensional horizontal distance, η is the elevation of the free surface above the x-axis datum (see Fig. 1a), and η_0 is the free-surface elevation at the upstream end section. As can be seen, the free-surface profiles are only self-similar in the flow region upstream from the axis of symmetry of the crest ($X < 1.5$). For this region, the free-surface profile can be described by a hyperbolic-tangent equation as

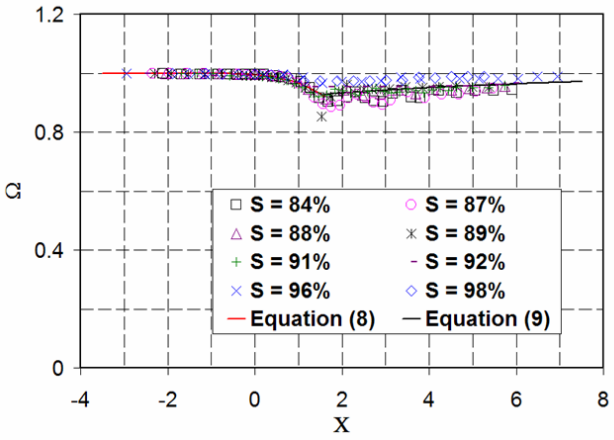

Fig. 7. Normalized free-surface profiles $\Omega(X)$ for various values of submergence ratio S. The results were based on the data of the test series of the three models from Zerihun's (2004) experiments

$$\Omega(X) = 0.910 - 0.098 \tanh\left(\frac{X - 1.727}{1.096}\right), \qquad X < 1.5. \tag{8}$$

Over the downstream face, the profiles do not exhibit self-similarity as in the case of the profiles of free flow over a trapezoidal broad-crested weir (see, e.g., Sargison and Percy 2009). The level of the tailwater strongly influences the dynamic characteristics of the submerged flow over the downstream face of the weir (Fritz and Hager 1998, Zerihun 2004). For a deeply submerged-flow situation, the weir flow becomes a hydrostatic free-surface flow with $\Omega(X) \cong 1.0$. In contrast to the above flow profile characteristics, the free overflow profiles of a trapezoidal short-crested weir show self-similarity throughout the sub- and super-critical flow regimes, as demonstrated

by Zerihun (2020). For the flow region downstream from the axis of symmetry of the crest, the normalized free-surface profile is approximately represented by

$$\Omega(X) = 1.0 - 0.093\exp(-0.155X), \qquad X \geq 1.5. \tag{9}$$

4.2. Bed-Pressure Distributions

Using the experimental data of Zerihun (2004), the effect of submergence on the streamwise variation of bed pressure was examined here. Fig. 8 shows the variation of the normalized bed-pressure profiles, $\xi = p_b/\gamma\eta_0$ (p_b is the bed pressure), with the normalized horizontal distance $X_w(= x/w)$. For the flow situation considered, the bed pressure is nearly constant in the transverse direction. Therefore, all bed-pressure measurements were taken along the centerline of the trapezoidal-shaped weir. For flow with a submergence ratio close to one ($S \cong 1.0$), the results clearly reveal a hydrostatic

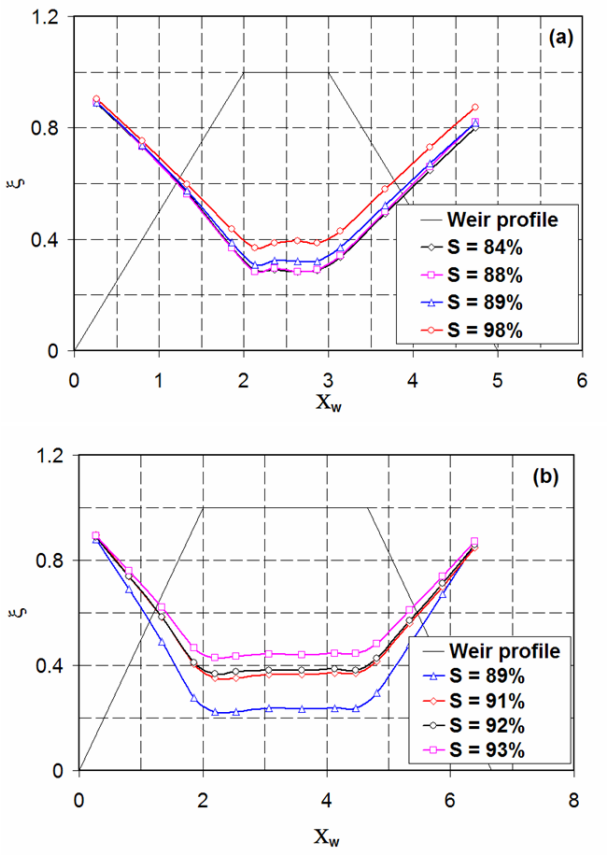

Fig. 8. Variation of the normalized bed pressure ξ with the normalized horizontal distance X_w for various values of submergence ratio S. The experimental data are from the test series of Models (a) Pn15 and (b) Pn40

bed-pressure distribution throughout the subcritical flow regime. A similar result was also reported by Pinto and Ota (1980) for the distribution of pressure on the downstream face of a submerged dike. For submerged flows over a trapezoidal-shaped weir with the slopes of the upstream and downstream faces flatter than 27°, the relative minimum bed pressure occurs at tapping points located on the weir crest. As noted by Zerihun and Fenton (2007), the internal structure of the submerged flow over the weir is strongly influenced by the degree of submergence. Hence, its minimum value depends on the submergence ratio of the quasi-hydrostatic flows (see Fig. 8). Compared to this, the bed-pressure profile of a short-crested weir under free-flow conditions has one absolute minimum pressure near the downstream edge of the weir crest due to the effects of the sharp curvature of the streamline (Zerihun 2020). The result of this analysis confirmed that the bed-pressure profiles exhibit self-similarity only over the upstream face of the weir (see Fig. 9).

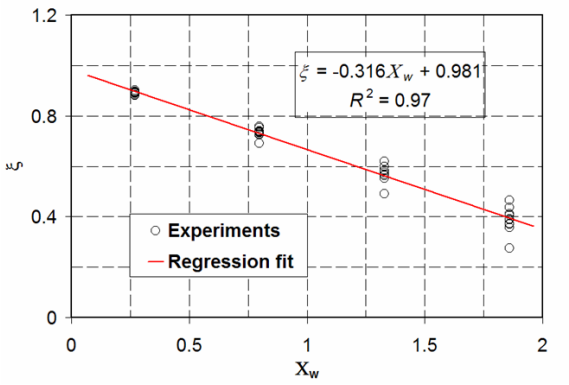

Fig. 9. Correlation between the normalized bed pressure and the dimensionless horizontal distance for flow over the upstream face of the weir

5. Conclusions

In this study, the most prominent characteristics of subcritical flows over trapezoidal-shaped weirs with sharp-crested edges have been systematically investigated using a large set of experimental data from the literature. Additionally, the momentum principle in a streamwise direction was applied to develop the equation of the submerged-flow discharge. Compared to earlier equations (e.g., Prawel 1958, Fritz and Hager 1998, Zerihun 2004, Hakim and Azimi 2017), the proposed equation does not require a pre-determined discharge under free-flow conditions. For simplifying the numerical computation, empirical equations for parameters σ and h_m/h were proposed as being valid for subcritical flows with the ranges of parameters provided in Table 1. Such a constraint restricts the range of application of the non-modular discharge equation. This equation was first calibrated and then validated using available measured

data. Its predictions were also compared with the results of an earlier semi-empirical equation (Skogerboe et al 1966). The results of the validation confirmed that the equation is capable of predicting the submerged-flow discharge of a trapezoidal-shaped weir within an error bound of ±6%. Compared to the semi-empirical equation, its overall performance is marginally better.

The analysis of the pressure data demonstrated that for a trapezoidal-shaped weir with face slopes flatter than 27°, the relative minimum bed pressure occurs on the crest of the weir due to the inconsequential effects of the small vertical acceleration of the overflow. For the submerged-flow situation considered, the free-surface and bed-pressure profiles are self-similar only over the upstream face of the weir. Based on the results obtained, it can be concluded that the degree of submergence and the slope of the downstream weir face significantly affect the characteristics of the submerged overflow. However, the effect of the downstream slope on the non-modular discharge is marginal. Finally, this study attests that the proposed equation can be applied to determine the submerged-flow discharge of a highway embankment or a levee that has been overtopped by flood waters.

Acknowledgments

The author would like to express his sincere appreciations to the staff of the Library of the Massachusetts Institute of Technology at Boston for providing a research report which contains relevant data for verifying the model.

References

Abou-Seida M. M., Quraishi A. A. (1976) A flow equation for submerged rectangular weirs, *Proc. Instn. Civ. Eng.*, **61** (4), 685–696.

Biegowski J., Paprota M., Sulisz W. (2020) Particle image velocimetry measurements of flow over an ogee-type weir in a hydraulic flume, *Int. J. Civ. Eng.*, **18**, 1451–1462.

Bos M. G. (1989) *Discharge Measurement Structures*, 3rd rev. ed., International Institute for Land Reclamation and Improvement: Wageningen, The Netherlands.

Curtis K. W. (2016) *Size-Scale Effect on Linear Weir Hydraulics*, Master's Thesis, Utah State University, Logan, UT, USA.

Fritz H. M., Hager W. H. (1998) Hydraulics of embankment weirs, *J. Hydraul. Eng.*, **124** (9), 963–971.

Hager W. H. (1994a) Breitkroniger überfall (Broad-crested weir), *Wasser Energie Luft*, **86** (11–12), 363–369 [in German].

Hager W. H. (1994b) Dammüberfälle (Dam overflows), *Wasser und Boden*, **45** (2), 33–36 [in German].

Hager W. H., Schwalt M. (1994) Broad-crested weir, *J. Irrig. Drain. Eng.*, **120** (1), 13–26.

Hager W. H. (2010) *Wastewater Hydraulics–Theory and Practice*, 2nd ed., Springer-Verlag, Berlin Heidelberg, Germany.

Hakim S. S., Azimi A. H. (2017) Hydraulics of submerged triangular weirs and weirs of finite-crest length with upstream and downstream ramps, *J. Irrig. Drain. Eng.*, **143** (8), doi:10.1061/(ASCE)IR.1943-4774.0001207.

Huang S. L., Ng C.-O. (2007) Hydraulics of a submerged weir and applicability in navigational channels: Basic flow structures, *Int. J. Numer. Methods Eng.*,**69**, 2264–2278.

Karim R. A., Mohammed J. R. (2020) A comparison study between CFD analysis and PIV technique for velocity distribution over the standard ogee crested spillways, *Heliyon*, **6** (10), doi:10.1016/j.heliyon.2020.e05165.

Kindsvater C. E. (1964) *Discharge Characteristics of Embankment-Shaped Weirs, Geological Survey Water-Supply Paper 1617-A*, U.S. Government Printing Office, Washington, DC, USA.

Lasdon L. S., Fox R. L., Ratner M. W. (1974) Non-linear optimization using the generalized reduced gradient method, *Revue Fr. d'Automatique Inform. Rech. Opér.*, **3** (8), 73–103.

Pedersen Ø., Fleit G., Pummer E., Tullis B. P., Rüther N. (2018) Reynolds-averaged Navier-Stokes modeling of submerged ogee weirs, *J. Irrig. Drain. Eng.*, **141** (1), doi:10.1061/(ASCE)IR.1943-4774.0001266.

Peltier Y., Dewals B., Archambeau P., Pirotton M., Erpicum S. (2018) Pressure and velocity on an ogee spillway crest operating at high head ratio: Experimental measurements and validation, *J. Hydro-Environ. Res.*, **19**, 128–136.

Pinto N.-L. de S., Ota J. J. (1980) Distribuição das pressões na face de jusante das barragens de enrocamento submersas – Investigação experimental (Pressure distribution on the downstream face of submerged rockfill dams – Experimental investigation), *Em Procedimentos do dia IX Congresso Latinoamericano Hidráulica*, Mérida, Venezuela, 30 Junho – 4 Julho, 529–540 [in Portuguese].

Prawel S. P. (1958) *Discharge Characteristics of an Embankment-Shaped Weir*, Master's Thesis, Georgia Institute of Technology, Atlanta, GA, USA.

Qian S., Zhang Y., Xu H., Wang X., Feng J., Li Z. (2021) Effects of surface roughness on overflow discharge of embankment weirs, *J. Hydrodynam.*, **33** (4), 773–781.

Rajaratnam N., Muralidhar D. (1969) Flow below deeply submerged rectangular weirs, *J. Hydraul. Res.*, **7** (3), 355–374.

Sargison J. E., Percy A. (2009) Hydraulics of broad-crested weirs with varying side slopes, *J. Irrig. Drain. Eng.*, **135** (1), 115–118.

Skogerboe G. V., Hyatt M. L., Austin H. L. (1966) *Stage-Fall-Discharge Relations for Flood Flows over Highway Embankments*, Report PR-WR6-7, Utah Water Research Laboratory, College of Engineering, Utah State University, Logan, UT, USA.

Smith R. A. (1959) Calibration of a submerged broad-crested weir, *J. Hydraul. Div.*, **85** (HY3), 1–16.

Thomas W. A. (1966) *Discharge Coefficients for Submerged, Broad-Crested Weirs*, Master's Thesis, Massachusetts Institute of Technology, Boston, MA, USA.

Vennard J. K., Weston R. F. (1943) Submergence effect on sharp-crested weirs, *Eng. News-Rec.*, **130** (22), 814–816.

Zerihun Y. T. (2004) *A One-Dimensional Boussinesq-Type Momentum Model for Steady Rapidly-Varied Open-Channel Flows*, Ph.D. Thesis, Department of Civil and Environmental Engineering, The University of Melbourne, Vic, Australia.

Zerihun Y. T., Fenton J. D. (2007) A Boussinesq-type model for flow over trapezoidal profile weirs, *J. Hydraul. Res.*, **45** (4), 519–528.

Zerihun Y. T. (2020) Free flow and discharge characteristics of trapezoidal-shaped weirs, *Fluids*, **5** (4), doi:10.3390/fluids5040238.